

Lattice anomalies in the FeAs_4 tetrahedra of the $\text{NdFeAsO}_{0.85}$ superconductor that disappear at T_c

M. CALAMIOTOU¹, I. MARGIOLAKI², A. GANTIS¹, E. SIRANIDI³, Z.A. REN⁴, Z.X. ZHAO⁴, AND E. LIAROKAPIS³

¹ *Solid State Physics Department, School of Physics, University of Athens, GR-15784 Athens, Greece*

² *ESRF, BP 220, Grenoble, Cedex 9, F-38043 France*

³ *Department of Physics, National Technical University of Athens, 157 80 Athens, Greece*

⁴ *National Laboratory for Superconductivity, Institute of Physics and Beijing National Laboratory for Condensed Matter Physics, Chinese Academy of Sciences, P.O.Box 603, Beijing, China*

PACS 74.70.-b – Superconducting materials
PACS 74.70.Xa – Pnictides and chalcogenides
PACS 61.05.cp – X-ray diffraction

Abstract. - High resolution synchrotron X-ray powder diffraction (SXRPD) was used to study the temperature dependence of the oxygen deficient $\text{NdFeAsO}_{0.85}$ superconducting compound. By employing a dense temperature sampling we have managed to reveal unnoticed structural modifications that start around $\sim 180\text{K}$, and disappear at the transition temperature. The data show minor changes of the structural characteristics in the Nd-O charge reservoir layer while in the superconducting Fe-As layer the FeAs_4 tetrahedron shows gradual modifications below $\sim 180\text{K}$, which suddenly disappear at T_c strongly indicating a connection with superconductivity.

Introduction. – The discovery of superconductivity in iron-based layered compounds $\text{REFeAsO}_{1-x}\text{F}_x$ (RE=Sm, Nd, Ce, Pr, Gd) belonging to the family of oxypnictides [1] attracted a lot of experimental and theoretical attention. However the mechanism, which induces superconductivity by doping the parent REFeAsO compound, is still controversial. REFeAsO has been found to undergo a structural tetragonal-to-orthorhombic phase transition upon cooling [2–4] and exhibits a spin density wave antiferromagnetic (AF) ordering [2, 5–7] closely resembling the cuprates. Both phenomena seems to be suppressed by doping and with the appearance of superconductivity. However in the hole-doped $\text{Nd}_{1-x}\text{Sr}_x\text{FeAsO}$ superconducting compound the structural phase transition is not suppressed by increasing the Sr^{2+} content [8]. In the oxygen deficient superconducting compound $\text{REFeAsO}_{1-\delta}$ [9] with T_c ranging from 31.2K for RE=La to 55K for RE=Sm and $\delta=0.15$, the tunable oxygen content leads to the occurrence of superconductivity strongly resembling the situation in cuprate superconductors.

Low temperature Fourier Transform Infrared (FTIR) studies in one of the highest T_c (53.5K) pnictides ($\text{NdFeAsO}_{0.85}$ [9]) have revealed unexpected spectral modifications and temperature dependent anomalies for cer-

tain modes at $\sim 180\text{K}$ [10]. Some marginal evidence of inflection points near T_c in the temperature dependence of the bond angle $\alpha_{\text{As-Fe-As}}$ and bond length $d_{\text{Fe-As}}$ has been recently reported for a $\text{NdFeAsO}_{0.85}$ sample [11]. In addition a femtosecond spectroscopy study of a single crystal $\text{SmFeAsO}_{0.8}\text{F}_{0.2}$ superconducting sample revealed the presence of a *pseudogaplike* feature with an onset above 180K [12]. Moreover, in the non-superconducting $\text{LaFeAsO}_{1-x}\text{F}_x$ a clear lattice anomaly has been detected at $\sim 180\text{K}$ that disappears upon AF ordering [13]. Detailed and accurate structural studies as a function of temperature are therefore essential in order to establish a clear picture of any correlation between crystal and electronic structures in the iron based superconductors. We present here high resolution synchrotron powder diffraction results as a function of temperature from the superconducting $\text{NdFeAsO}_{0.85}$ system ($T_c=53.5\text{K}$) [9]. Our data recorded with a dense sampling in the temperature range down to 10K provide clear evidence of subtle lattice distortions that start at $T_{\text{onset}} \approx 180\text{K}$ and disappear at T_c .

Experimental. – We have collected SXRPD data on beamline ID31 at the European Synchrotron Radiation Facility (ESRF), Grenoble, France. The experimental set-

up is described in detail elsewhere [14]. The short wavelength ($\lambda = 0.39998(5)\text{\AA}$), to reduce absorption, was selected with a double-crystal Si(111) monochromator and calibrated with Si NIST standard. Optimum transmission was achieved by enclosing the finely ground sample in a 0.6mm diameter borosilicate glass capillary and appropriate spinning of the capillary in the beam ensured for a good powder averaging. An exchange gas continuous liquid-helium flow cryostat with rotating sample rod was used to cool the sample down to 10K. High statistics high resolution diffraction patterns ($2\theta = 1 - 53^\circ$, d spacing $22.9\text{\AA}-0.45\text{\AA}$, 0.004° step, scan time 30min) have been recorded at selected characteristic temperatures. High resolution diffraction patterns (short scans with $2\theta = 1 - 33^\circ$, d spacing $22.9\text{\AA}-0.7\text{\AA}$, 0.004° step and scan time 1min), were also collected upon heating (thermodiffractograms) from 10K up to 295K in order to follow the evolution of the lattice constants and interatomic distances with a dense temperature sampling. Due to the short time interval of the short scans upon heating the *c*-axis values show that there was an $\sim 10\text{K}$ difference between the nominal and the actual value of temperature. Therefore, all temperature values of the short scans are shifted in the following plots by this amount to lower values.

Data analysis has been performed with the GSAS+EXPGUI suite of Rietveld analysis programs [15] assuming the tetragonal (SG P4/nmm) structure for the NdFeAsO_{0.85} phase. The pseudo-Voigt function corrected for asymmetry owing to axial divergence and anisotropic broadening was used for the peak profile (profile No 4 in GSAS [16]). The data have been sequentially refined starting from the diffraction pattern recorded at 10K. The high statistics diffraction patterns, collected at the characteristic temperatures, have been used to fully refine the values of the profile parameters, the Nd and As coordinates and the atomic displacement factors U_{iso} of NdFeAsO_{0.85}. Oxygen occupancy has been fixed to the nominal value, justified by the agreement of the Nd-As bond length value to that obtained from a neutron diffraction study in a series of variable oxygen stoichiometry NdFeAsO_{1-y} samples [17]. The refinements take into account small amounts of the impurity phases FeAs ($5\pm 0.9\%$ wt) and Nd₂O₃ ($1.4\pm 0.3\%$ wt) while a few very weak peaks due to other minor impurity phases ($< 0.1\%$ wt) have been excluded. We note that excluding also the peaks of the two main impurity phases does not affect the structural results.

Results and discussion. – Figure 1 shows the diffraction pattern at 10K together with the result of the Rietveld refinement. The high resolution data reveal no splitting or broadening of the 110 reflection profiles that would be the sign of a tetragonal-orthorhombic (T-O) phase transition down to 10K, as shown in the inset in Fig.1. Table I shows the structural parameters at different temperatures obtained from the Rietveld refinement of the high statistics patterns. The position of the As

atom does not change in the whole temperature range examined. The fractional coordinate of the Nd atom along the *c*-axis remains constant down to 140K, it jumps to a higher value within 140-60K, indicating that the Nd atom shifts closer to the superconducting Fe-As layer, and then it remains practically constant to the lowest temperature studied. The thermodiffractograms between the characteristic temperatures have been analyzed using both the Rietveld and the LeBail (whole-powder pattern decomposition method not based on the structural model) method. Minor impurity peaks were excluded from the refinement. The Rietveld analysis has been performed combined with the high statistics data, i.e., the atomic positions and the atomic displacement factors U_{iso} were fixed to the corresponding values obtained from the refinements of the high statistics data. In the temperature region 60K-140K, where the fractional coordinate of the Nd atom has been found to exhibit a change, we have assumed a smooth linear change of *z*. The LeBail refinement, not based on a specific structural model, resulted to identical values of the lattice constants.

The temperature dependence of the *c*- and *a*-axis (Fig.2) reveals two important features: a slope change at $T\sim 180\text{K}$ and a subtle anomaly at T_c . The lattice of NdFeAsO_{0.85} contracts anisotropically, the relative change being $\Delta a/a=0.136\%$ and $\Delta c/c=0.37\%$ from 295K to 60K, in agreement with previous reports [11]. The distance between two adjacent Nd and As atoms that reflects the spacing between the charge reservoir Nd-O and the superconducting Fe-As layer (Fig.3a), decreases from 295K to 60K by 0.235% following the reduction of the *c*-axis. The Nd-O bond contracts upon cooling (0.159%) following the contraction of the *a*-axis (Fig.3b), while the Nd-O-Nd bond angle exhibits only marginal changes with temperature (Fig.3c). On the contrary, the Fe-As bond length in the superconducting layer exhibits a bigger change (0.235%) comparable to that of the *c*-axis (Fig.4a). The tetrahedral bond angle $\alpha_{\text{As-Fe-As}}$ (Fig.4b) is increasing while $\beta_{\text{As-Fe-As}}$ (Fig.4c) is decreasing, indicating an increase of tetrahedral distortion with decreasing temperature. The FeAs₄ coordination tetrahedron is distorted from the ideal symmetry. Robinson *et al* [18] have found that a quantitative measure of the distortion in such a case is the variance of the tetrahedral angle expressed as

$$\sigma^2 = \sum_{i=1}^6 (\theta_i - 109.47^\circ)^2 / 5$$

where θ_i are the bond angles of the distorted tetrahedron and 109.47° the corresponding one in an ideal tetrahedron. Fig.5a shows the distortion of the Fe coordination tetrahedron and Fig.5b presents the temperature evolution of the volume [19] of the FeAs₄ tetrahedra in comparison to that of the cell volume both normalized to their values at 295K.

The temperature evolution of all structural features (Figs.2-5) reveals anomalies at characteristic temperatures. Specifically, at $T_{\text{onset}}\sim 180\text{K}$ a change of slope is evident in the lattice constants (Fig.2), the inter-layer

Nd-As distance (Fig.3a), the intra-layer Nd-O bond length (Fig.3b) and angle (Fig.3c), as well as in the geometrical characteristics of the FeAs₄ tetrahedra (Figs.4,5). This change is much more pronounced in the superconducting Fe-As layer. Furthermore, around T_f~135K, a modification in the temperature dependence is evidenced for all bond length characteristics (Figs.3-5). It looks like a new order parameter coupled to the lattice and mostly to the Fe-As tetrahedra sets in at T_{onset} which is completed at T_f (Figs.4-5). At T_c the Fe-As bond length and the distortion of the FeAs₄ tetrahedra exhibit a sudden change (Figs.4-5) while the Nd-O bond length and angle values saturate (Fig.3). The modifications around T_c are not so pronounced in the charge reservoir planes being less sensitive to changes with temperature. The structural data indicate a bigger effect in the superconducting Fe-As planes. The relative contraction of the FeAs₄ volume deviates in a profound way from that of the unit cell below T_{onset} where the angle distortion is also modified. Crossing T_c the anomalies are obviously reduced (Fig.5).

The lattice distortions appear below ~180K where certain IR modes exhibit an anomalous behavior in the same compound [10]. The non-superconducting undoped Nd-FeAsO compound is known to exhibit a tetragonal to orthorhombic phase transition that starts at 150K [4], and a magnetic ordering of the iron spins below ~141K [7]. One could assume that the lattice anomaly observed in the region 180K-T_c, originates from a T-O structural phase transition because such a phase transition can be traced in other superconducting oxypnictides [3, 8]. However our high resolution diffraction data (inset in Fig.1) do not support such possibility. On the other hand the iron spins could order antiferromagnetically along the c-axis at ~141K [7], but this phase should be absent in the optimally doped compound, though it may be present at low doping levels [20, 21]. The assumption of two chemically separated phases cannot be justified from the XRD results since no splitting or broadening of the xrd peaks was observed. However, a mesoscopic phase separation cannot be excluded, at least in the underdoped pnictides [21]. The observation of similar lattice distortions that start below ~180K and relaxes at T_N in the non-supeconducting LaFeAsO_{1-x}F_x [13] and the appearance of a new photo-induced reflectivity component in the superconducting SmFeAsO_{0.8}F_{0.2} [12] point to a lattice distortion effect of common origin in all these pnictides. But while in the non-superconducting compound with the AF ordering the effect disappears at T_N, in the photo-induced reflectivity results that probe the electronic states the component remains into the superconducting state, and in our structural data of superconducting compound the lattice distortions are relaxed at T_c. It appears that another order parameter, which is common to all compounds sets-in around T_{onset} and affects spin, lattice, and electronic states.

Based on the Fe-As₄ angle modifications (Fig.5a) one could assume local distortions that involve orbital order-

ing in the Fe planes. Martinelli et al [22] have proposed that the structural transition could originate by this distortion that brings a similarity of the oxypnictide systems to the manganites. At T_{onset} both the volume and the distortion of the FeAs₄ tetrahedra show an anomaly that saturates at T_f and disappears below T_c. The direct effect on the lattice and more precisely the anomalous contraction of the volume of the FeAs₄ tetrahedra (Fig.5b) and the increase of their distortion indicates a polaronic mechanism. In such a case, the polarons should start been formed around 180K. In the undoped compound the polarons could be related with the AF ordering [13]. In the presence of carriers, the AF ordering is suppressed and the instability remains down to T_c (Fig.5b). The return of the volume of the FeAs₄ tetrahedron (Fe-As bond length) below T_c to the anticipated value from the high temperature data could be due to the delocalization of the polarons in the superconducting phase. Whatever happens our data show that there are modifications of the c-axis at T_{onset} and T_c (Fig.2), and indicate that the lattice effects occur mainly within the FeAs₄ tetrahedra and are related with the carriers and possibly with superconductivity. Anomalies observed at similar temperatures indicate that this might be a general feature of these compounds and reserve further investigation on all pnictides.

In conclusion, the high resolution synchrotron diffraction data collected with dense sampling in the temperature range 10-295K revealed the presence of subtle lattice anomalies, which coincide with those in the IR modes at ~180K and disappear at the critical temperature. These lattice anomalies, apparently not connected with a structural phase transition, are more evident in the superconducting Fe-As planes consisting of a distortion and contraction of the FeAs₄ tetrahedra and a reduction of the Nd-As distance indicating charge transfer. The disappearance of the anomaly across T_c points to a connection to superconductivity.

We thank the ESRF for providing synchrotron beam time at ID31 instrument and Dr. Larry Finger for his advice with respect to the use of program DRAWxtl.

REFERENCES

- [1] Y. Kamihara, T. Watanabe, M. Hirano, H. Hosono, *J.Am.Chem.Soc.* **130** (2008) 3296 .
- [2] T. Nomura, S.W. Kim, M. Hirano, P.V. Sushko, K. Kato, M. Takata, A.L. Shluger, and H. Hosono, *Supercond. Sci.Technol.* **21** (2008) 125028 .
- [3] S. Margadonna, Y. Takabayashi, M.T. McDonald, M. Brunelli, G. Wu, R.H. Liu, X.H. Chen, and K. Prassides, *Phys. Rev. B* **79** (2009) 014503 ; A. Martinelli, A. Palenzona, C. Ferdeghini, M. Putti, and H. Emerich, *J. All. Comp.* **477** (2009) L21 .
- [4] M. Fratini, *Supercond. Sci.Technol.* **21**(2008) 092002 .

- [5] J. Dong, *Europhys. Lett.* **83** (2008) 27006 .
- [6] C. Cruz, Q. Huang, J.W. Lynn, J. Li, W. Ratecliff II, J.L. Zarestky, H.A. Mook, G.F. Chen, J.L. Luo, N.L. Wang, and P. Dai, *Nature* **453** (2008) 899 .
- [7] Y. Chen, J.W. Lynn, J. Li, G. Li, G.F. Chen, J.L. Luo, N.L. Wang, Pengcheng Dai, C. dela Cruz, H.A. Mook, *Phys. Rev. B* **78**(2008) 064515 .
- [8] K. Kasperkiewicz, J.W.G. Bos, A.N. Fitch, K. Prassides, and S. Margadonna, *Chem. Commun.*, Issue 6 (2009) 707 . DOI: 10.1039/B815830D(2009).
- [9] Z.A. Ren, G.C. Che, X.L. Dong, J. Yang, W. Lu, W. Yi, X.L. Shen, Z.C. Li, L.L. Sun, F. Zhou, and Z.X. Zhao, *Europhys.Lett.* **83** (2008) 17002.
- [10] E. Siranidi, D. Lampakis, E. Liarokapis, Z. Dohcevic-Mitovic, N. Paunovic, Z.V. Popovic, and Z.X. Zhao, *J. Alloys and Comp.* **487**(2009) 430.
- [11] R. Kumai, T. Ito, H. Kito, A. Iyo, and H. Eisaki, *J. Phys. Soc. Jpn.* **77**,Suppl. C (2008) 134.
- [12] T. Mertelj, V.V. Kabanov, C. Gadermaier, N.D. Zhigadlo, S. Katrych, J. Karpinski, and D. Mihailovic, *Phys. Rev. Lett.* **102** (2009) 117002.
- [13] N. Qureshi, et al., arXiv:1002.4326v1 (2010).
- [14] A.N. Fitch, *J. Res. Natl. Instr. Stand. Technol.* **109**(2004) 133.
- [15] A.C. Larson, and R.B. von Dreele, *General Structure Analysis System (GSAS)*, Los Alamos National Laboratory Report LAUR,(1994) p.86-748 ;B.H. Toby, *EXPGUI*, *J. Appl. Cryst.* **34** (2001) 210-213
- [16] P. Stephens, *J. Appl. Cryst.* **32**(1999) 281.
- [17] C.H. Lee *et al.*, *J. Phys. Soc. Jpn.* **77**(2008) 083704.
- [18] K. Robinson, G.V. Gibbs, and P.H. Ribbe, *Science* **172** (1971) 567.
- [19] L.W. Finger, M. Krokner, and B.H. Toby, *J. Appl. Cryst.***40** (2007) 188 .
- [20] M. Rotter, M. Tegel, I. Schellenberg, F.M. Schappacher, R. Pöttgen, J. Deisenhofer, A. Günther, F. Schrettle, A. Loidl, and D. Johrendt, *New Journal of Physics* **11**, 025014 (2009).
- [21] J.T. Park, D.S. Inosov, Ch. Niedermayer, G.L. Sun, D. Haug, N.B. Christensen, R. Dinnebier, A. V. Boris, A.J. Drew, L. Schulz, T. Shapoval, U. Wolff, V. Neu, Xiaoping Yang, C.T. Lin, B. Keimer, and V. Hinkov, *Phys. Rev. Lett.* **102**, 117006 (2009).
- [22] A. Martinelli, A. Palenzona, M. Tropeano, C. Ferdeghini, M.R. Cimberle, and C. Ritter, *Phys. Rev. B* **80**(2009) 214106 .

FIGURE CAPTIONS. – Figure 1. Experimental (circles), calculated (continuous line) SXRPD patterns and their difference (bottom line) at T=10K. Bars indicate the theoretical Bragg peak positions for NdFeAsO_{0.85}. The two lower rows of bars indicate the Bragg peak positions of the impurity phases FeAs and Nd₂O₃ respectively. The inset shows the profiles of the 110 reflection at different temperatures. Intensities are scaled to the most intense line in the spectrum I_{max} and peaks are shifted to be superimposed.

Figure 2. The dependence of the c- and a-axis on temperature. Full circles: high statistics scans. Open trian-

gles: thermodiffractograms. Errors are smaller than symbols.

Figure 3. The change of (a) the inter-layer distance between two adjacent Nd and As atoms, (b) the intra-layer Nd-O bond length, and (c) the Nd-O-Nd angle with temperature. Full circles: high statistics scans with estimated standard deviations (esd's). Open triangles: thermodiffractograms with error bars calculated on the basis of error propagation from the corresponding errors of lattice constants and atomic positions. Lines are polynomial fits to guide the eye.

Figure 4. Temperature evolution of the intra-layer Fe-As bond length (a) and Fe-As-Fe angles (b) and (c). Full circles: high statistics scans with esd's. Open triangles: thermodiffractograms with error bars calculated on the basis of error propagation from the corresponding errors of lattice constants and atomic positions.

Figure 5. Temperature evolution of (a) the tetrahedral distortion (angle variance), (b) the normalized volumes of FeAs₄ (circles and triangles) and unit cell (squares and crosses) to their values at 295K. Full circles: high statistics scans with esd's. Open triangles: thermodiffractograms with error bars calculated on the basis of error propagation from the corresponding errors of lattice constants and atomic positions.

Table 1: Rietveld refinements of synchrotron diffraction data for NdFeAsO_{0.85} at different temperatures. The space group is P4/nmm with Nd on $2c(\frac{1}{4}, \frac{1}{4}, z)$, Fe on $2b(\frac{3}{4}, \frac{1}{4}, \frac{1}{2})$, As on $2c(\frac{1}{4}, \frac{1}{4}, z)$, O on $2a(\frac{3}{4}, \frac{1}{4}, 0)$.

		T=10K	T=50K	T=60K	T=140K	T=160K	T=180K
Nd	z	0.14381(6)	0.14383(7)	0.14385(6)	0.14356(6)	0.14363(7)	0.14364(7)
	$U_{iso}(\text{x}100\text{\AA}^2)$	0.144(6)	0.131(7)	0.145(6)	0.279(7)	0.314(8)	0.293 (8)
Fe	$U_{iso}(\text{x}100\text{\AA}^2)$	0.18(2)	0.16(2)	0.26(2)	0.39(3)	0.39(3)	0.40(3)
As	z	0.6586(1)	0.6586(1)	0.6584(1)	0.6584(1)	0.6586(1)	0.6587(1)
	$U_{iso}(\text{x}100\text{\AA}^2)$	0.18(1)	0.16(2)	0.26(1)	0.38(1)	0.40(2)	0.40(1)
O	$U_{iso}(\text{x}100\text{\AA}^2)$	1.2(2)	1.6(3)	1.7(2)	1.5(2)	1.4(2)	1.4(2)
	a (Å)	3.94986(1)	3.94999(1)	3.95000(1)	3.95116(1)	3.95160(1)	3.95226(1)
	c (Å)	8.50360(4)	8.50479(4)	8.50467(4)	8.51228(5)	8.51525(5)	8.51899(5)
	R_{wp}	0.1094	0.1410	0.1357	0.1183	0.1209	0.1322
	$R(F^2)$	0.0951	0.1050	0.0817	0.884	0.0807	0.949

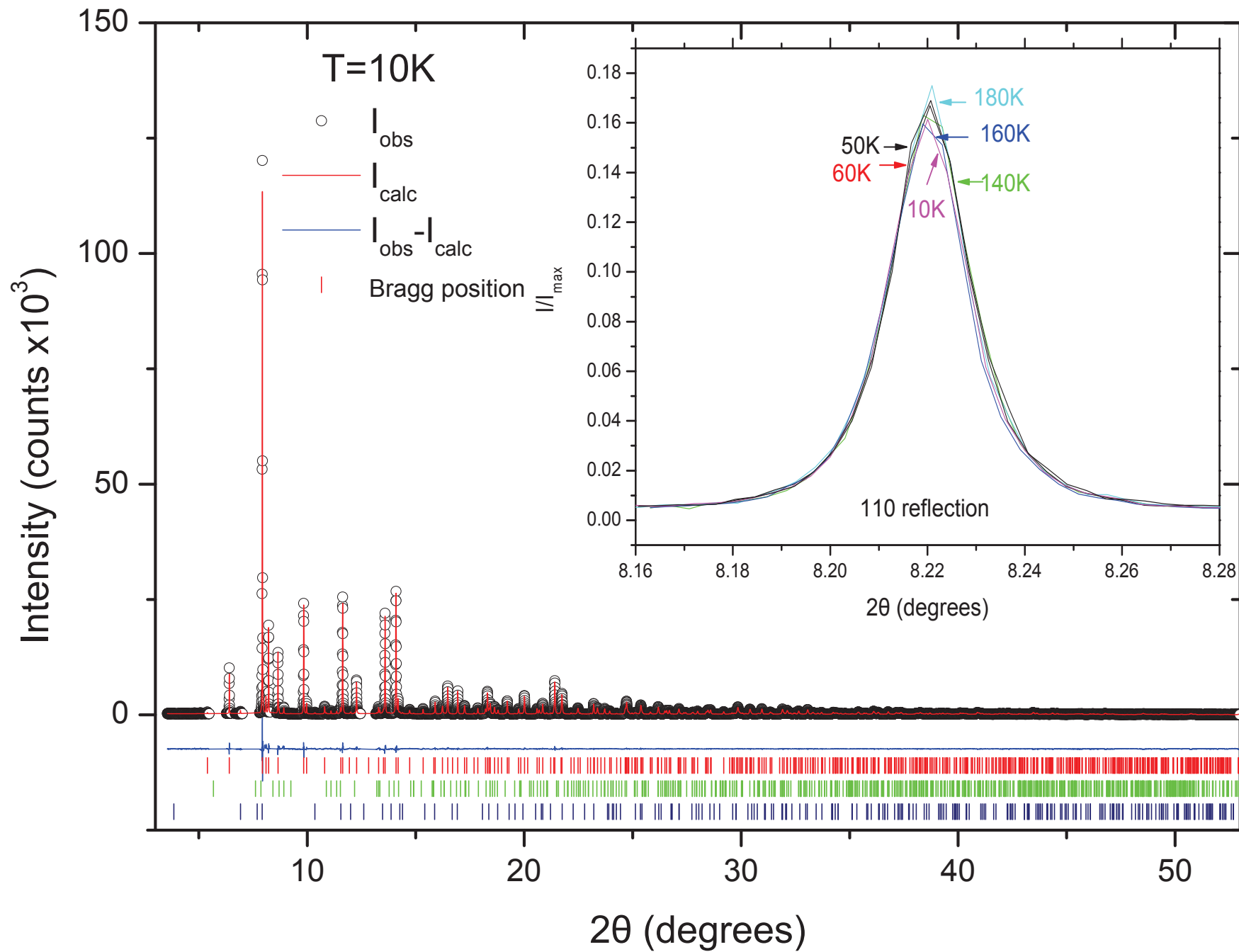


Figure 1

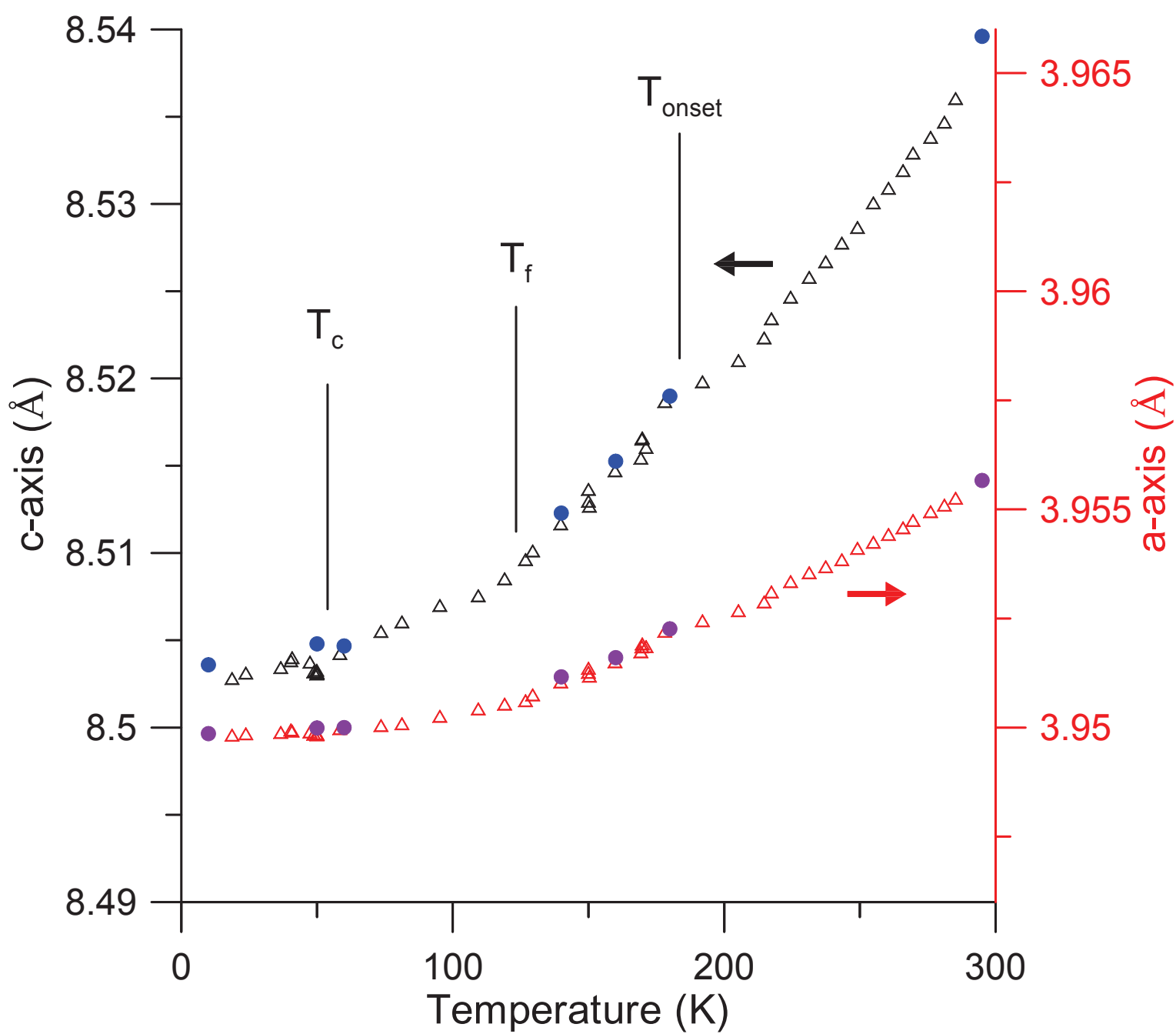


Figure 2

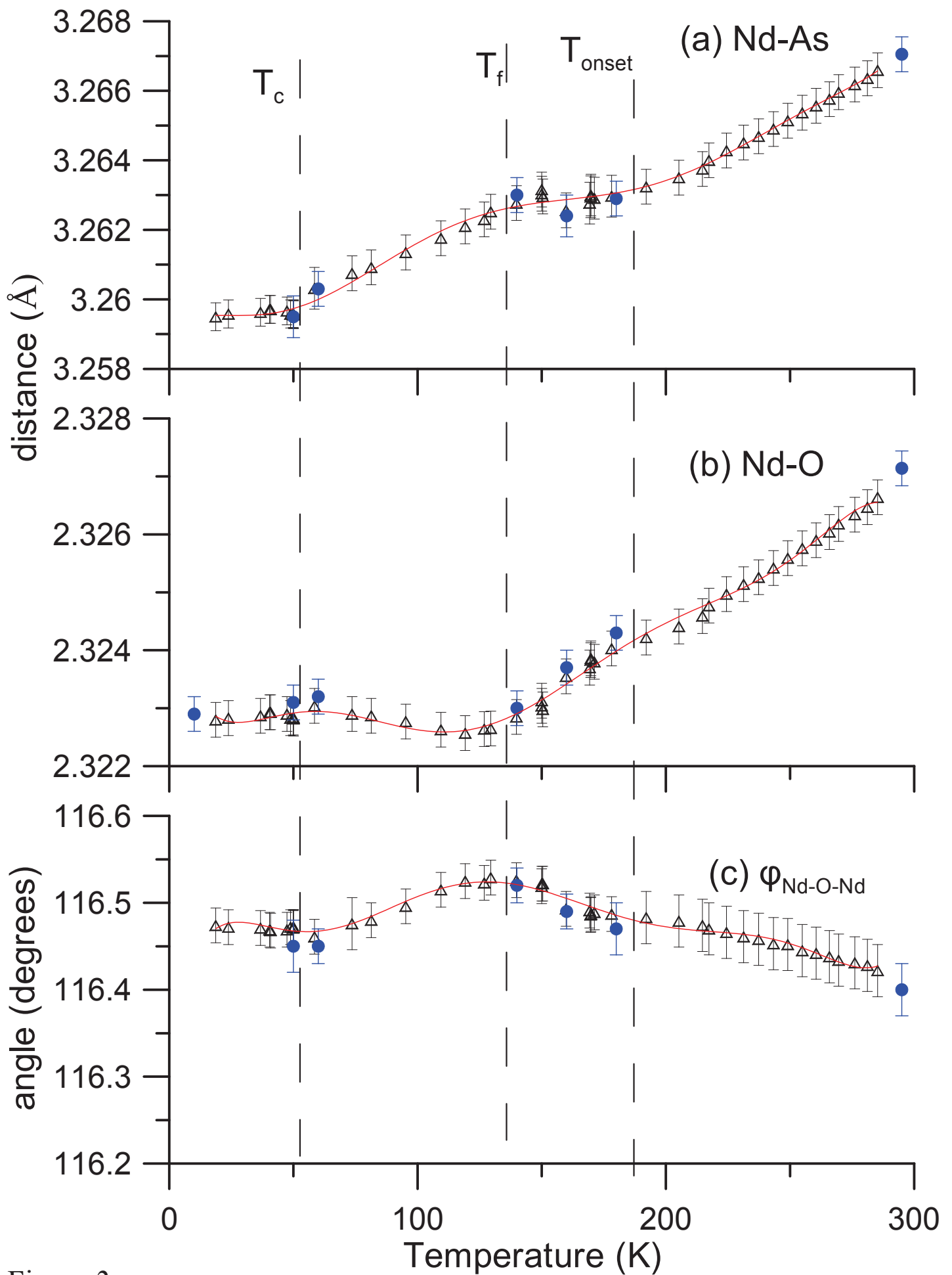


Figure 3

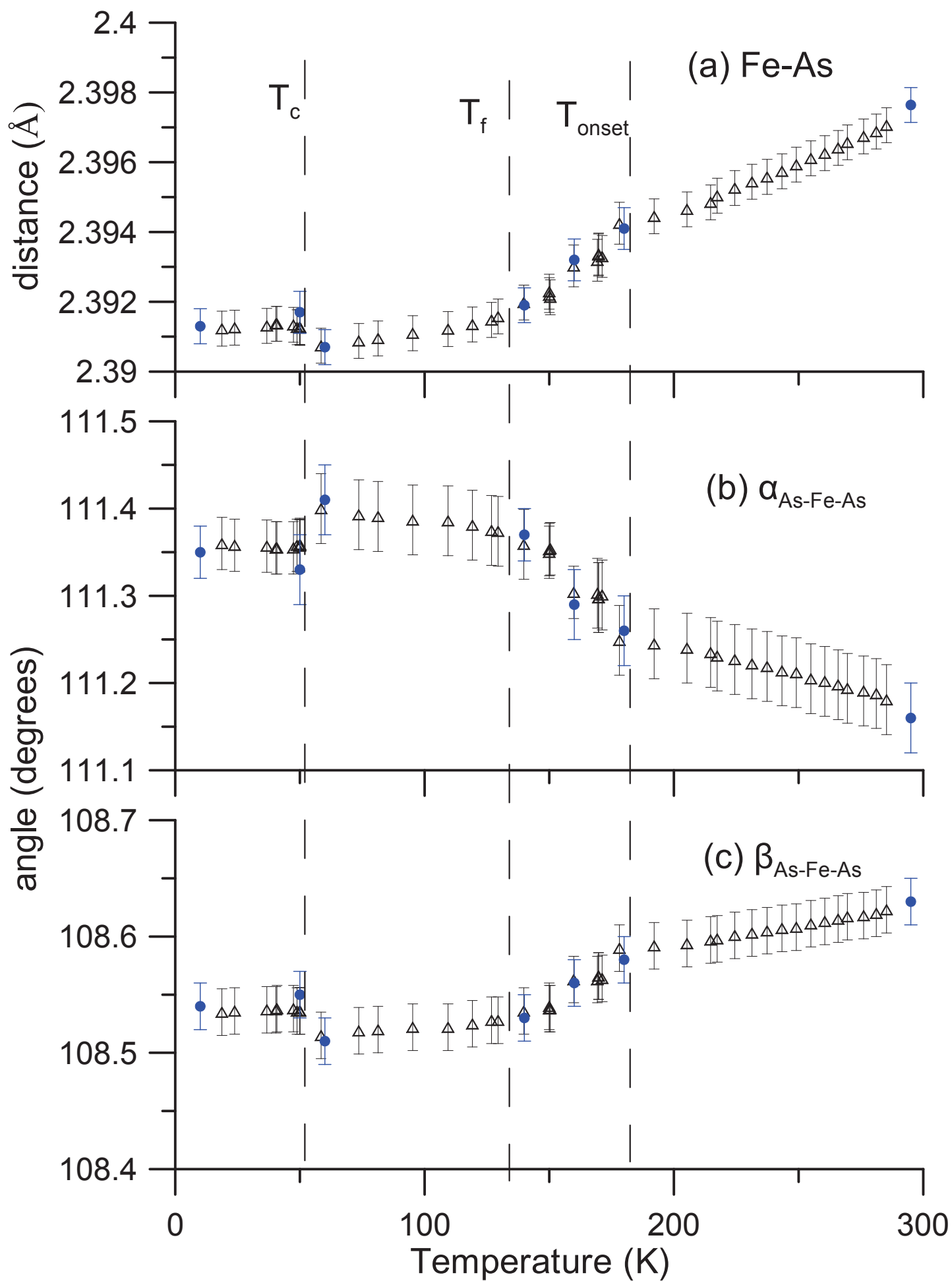


Figure 4

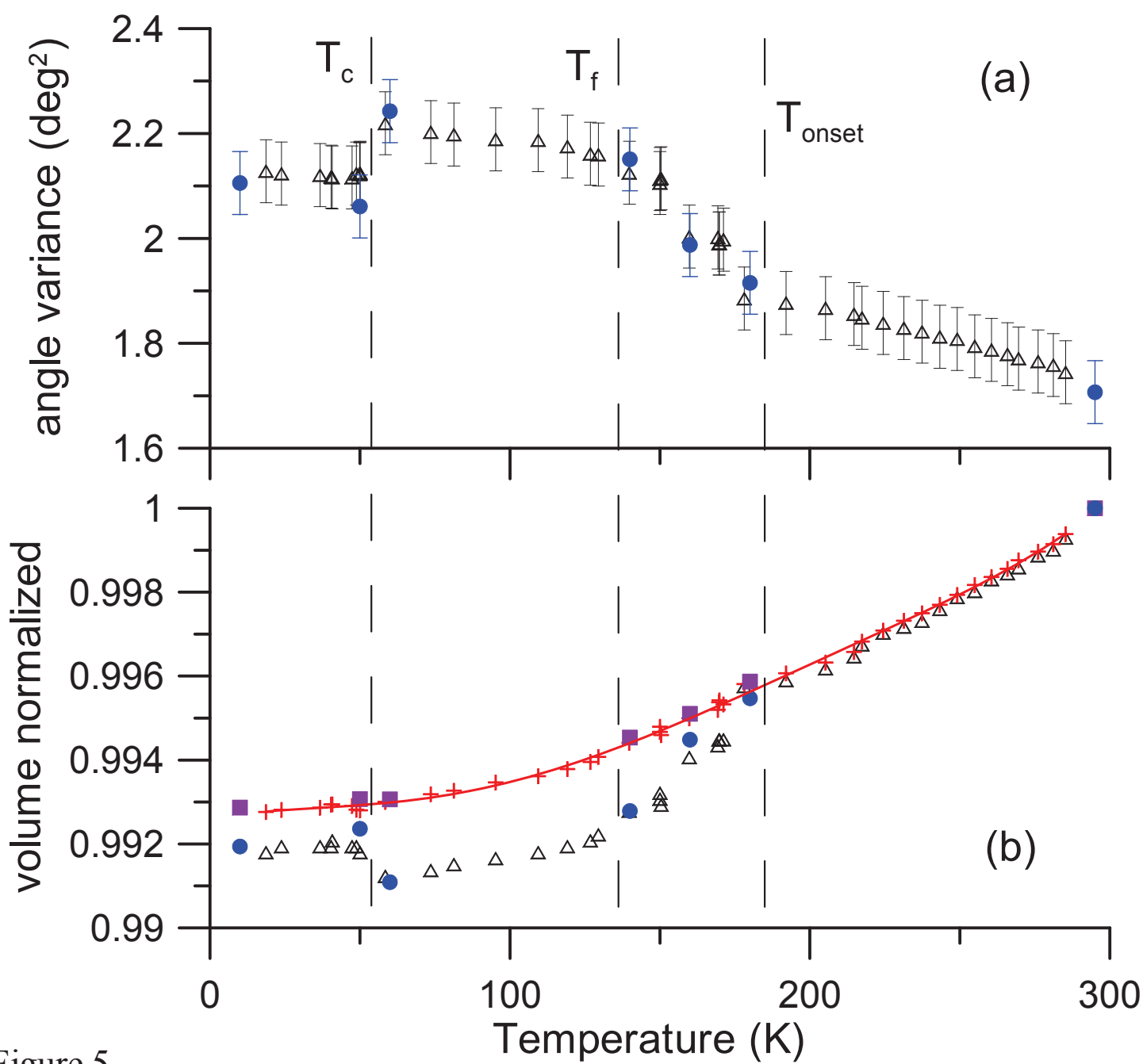


Figure 5